Contrib Mineral Petrol (2004) 147: 110–122
DOI 10.1007/s00410-003-0549-8

ORIGINAL PAPER

Jean-Louis Paquette · Philippe Goncalves
Bertrand Devouard · Christian Nicollet

Micro-drilling ID-TIMS U-Pb dating of single monazites: A new method to unravel complex poly-metamorphic evolutions. Application to the UHT granulites of Andriamena (North-Central Madagascar)

Received: 3 March 2003 / Accepted: 17 November 2003 / Published online: 20 January 2004

Abstract In terranes subject to complex metamorphic evolution, zircon and monazite U-Pb system can record successive growth and/or resetting episodes. Conventional isotope dilution-thermal ionisation mass spectrometry (ID-TIMS) dating of fractions or single grains from conventionally separated zircon and monazite populations may produce inaccurate ages. A new technique combining textural analysis and ID-TIMS dating on single monazite crystals is proposed. This method is applied directly on thin sections with three successive steps comprising (1) a characterisation of textural relationships using electron microprobe analyses and images, (2) extraction by micro-drilling of selected monazites and (3) U-Pb dating of each extracted grain by ID-TIMS. The potential for this "in situ" dating technique are tested on Ultra High Temperature (UHT) granulites from North-Central Madagascar. Four distinct events on a single thin section were distinguished. The UHT metamorphism was dated at 2.5 Ga, while two retrogression events were dated at 790 and 500 Ma. Finally, a single crystal shielded in quartz seems to preserve a pre-metamorphic age around 2.7 Ga.

Introduction

The monazite [$(Ce,La,Nd)PO_4$] is a common accessory mineral occurring in numerous magmatic and metamorphic rocks (e.g. Overstreet 1967). The high concentrations of U and Th make monazite relatively easy to date with the U-Th-Pb chronometer (Parrish 1990). However, monazite has also the potential to preserve inherited cores, record successive growth phases and/or partial resetting, yield discordant or reverse discordant age results, and incorporate common Pb or unsupported ^{206}Pb due to ^{230}Th desequilibrium (Schärer et al. 1986; Copeland and Parrish 1988; DeWolf et al. 1993; Harrison et al. 1995, 1999; Braun et al. 1998; Cocherie et al. 1998). This represents a critical point for the interpretation of U-Th-Pb dating results obtained by the currently available techniques on this mineral. The conventional isotopic dilution and thermal ionisation mass spectrometry method (ID-TIMS) applied to fractions or single grains of conventionally separated monazite populations can result in partly scattered discordant analytical points producing inaccurate intercept ages (Foster et al. 2002). Based on the occurrence of non-zero lower intercepts and various discordance levels, the Pb evaporation technique (Kober 1986 and 1987; Kouamelan et al. 1997) only indicates a wide range of minimum $^{207}Pb/^{206}Pb$ apparent ages. Consequently, it appears that monazite is very useful for unravelling complex geological histories, but it requires in-situ analyses with high-spatial resolution in order to distinguish on the one hand the various age domains at the crystal-scale and on the other hand the textural relationships between the monazites and their host minerals. This can be achieved by U-Th-Pb chemical dating using electron microprobe (EMP) on thin section (e.g. Montel et al. 1996). The advantages of this technique are well known: rapidity, lower cost and excellent spatial resolution (spot size $\approx$3 μm), the major drawback being a relative low precision on the ages. However, in case of discordant monazite, the dates obtained are only apparent ages. The most powerful tool for precise in situ dating is the high-resolution ion microprobe (SIMS), although laser ablation multi-collector inductively coupled plasma mass spectrometry (LA-MC-ICPMS) could provide in the future an alternative

Editorial responsibility: J. Hoefs

J.-L. Paquette (✉) · P. Goncalves · B. Devouard · C. Nicollet
Laboratoire Magmas et Volcans,
Université Blaise Pascal-CNRS,
5 rue Kessler, 63 038 Clermont-Ferrand,
France
E-mail: paquette@opgc.univ-bpclermont.fr
Fax: +33-0-473346744

P. Goncalves
Geosciences Department, University of Massachusetts,
611 North Pleasant Street, Amherst,
MA 01003-9297, USA

technique (Foster et al. 2002). The ion microprobe is mostly used on grain mounts of isolated handpicked monazites (Stern and Sanborn 1998; Zhu et al. 1997a and 1998; Stern and Berman 2001). Few laboratories are also studying and dating monazites in thin section (DeWolf et al. 1993; Zhu et al. 1997b; Foster et al. 2000; Catlos et al. 2002a, 2002b). The low amount of Pb provided by the ca. 10–30 μm spot size and some U-Pb calibration difficulties (i.e. Stern 1997) favoured the measurement of $^{207}Pb/^{206}Pb$ (Zhu et al. 1997b) and especially $^{208}Pb/^{232}Th$ ratios, and corresponding apparent ages. This last approach provided important age constraints, particularly on monazites containing inherited components (Harrison et al. 1995, 1999). However, the single $^{208}Pb/^{232}Th$ ratio itself cannot be plotted in a concordia diagram and consequently the concordancy (or discordancy) of the analyses remains difficult to estimate (Foster et al. 2000).

We developed a new technique of ID-TIMS dating on monazites micro-drilled from rock thin section previously analysed for electron microprobe. Each monazite dating technique has its own merits and drawbacks: EMP chemical [Th-Pb] dating provides high spatial resolution and low precision, whereas ID-TIMS provides high precision and low spatial resolution. The combination of both methods may merge the advantages of the "in-situ" analysis (at the scale of the micro-drilling) and the precision of ID-TIMS U-Pb geochronology, to better understand age results from a complexly metamorphosed terrane. Furthermore, the determination of the two U-Pb isotopic ratios (in addition to chemical [Th-Pb] age mapping) allows one to distinguish discordant monazites in the concordia diagram. This technique can be described as: (1) characterisation (i.e. textural relationships, chemical composition, and mapping of the EMP [Th-Pb] chemical ages) of monazites in thin sections; (2) extraction by micro-drilling of individual monazite grains (minimum size 60 μm wide); (3) dating of each individual extracted grain by ID-TIMS. An important aspect of this work is that EMP and ID-TIMS data were acquired from the same grains extracted by micro drilling directly from petrographic thin-sections.

Whatever the dating technique, the common selection of zircons and monazites is based on magnetic susceptibility, crystal morphology, colour and inclusions characteristics. In this study, monazite selection for isotopic analysis is based on the petrographical setting (i.e. included in peak metamorphic phases, associated with secondary assemblages, located in the matrix foliation or in pressure shadow). Because of its non-destructive nature and high spatial resolution, dating of monazite by EMP highlights key grains for subsequent isotopic dating and provides important structural and textural information for the interpretation of conventional dating results (Williams and Jercinovic 2002).

We applied this method to a polymetamorphic UHT (Ultra-High Temperature) granulite from the Andriamena unit, North-Central Madagascar. To constrain the magmatic and metamorphic evolution of the Andriamena unit and to compare the results obtained by the micro-drilling dating method, three samples have first been dated by conventional ID-TIMS dating on monazite and zircon separates. Attention has been paid to the influence of the textural position and the role of fluid composition on the variable degrees of discordance reported in U-Pb analysed monazites. Finally, we discuss the geological implications of the dating results and we estimate the timing of specific metamorphic assemblages and reactions.

Geological setting and petrography of sampled material

The Andriamena unit, located in the North-Central Madagascar (Fig. 1), is a Precambrian allochthonous

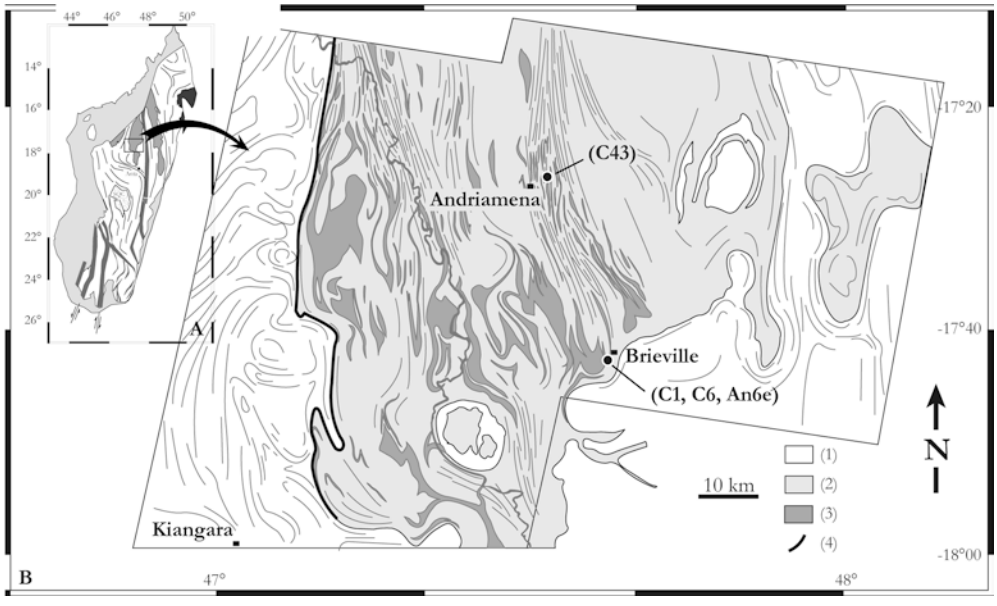

Fig. 1 **A** Simplified geological map of Madagascar, showing the location of the studied area. **B** Simplified geological map of a part of the Andriamena unit and the surrounding basement, with the main structural trends and sample location (C1, C6, C43 and An6e). *1* Reworked Archaean and Neoproterozoic gneissic and granitic basement; *2* The Andriamena unit-sequence of Archaean and Neoproterozoic tonalitic and granodioritic gneiss, interlayered metapelitic migmatites, quartzites, mafic gneisses; *3* Intrusive middle Neoproterozoic ultramafic and mafic rocks; *4* Cambrian mylonitic contact

mafic-ultramafic sequence that has experienced a complex tectono-metamorphic and igneous activity since late Archaean to Cambrian times (Guérrot et al. 1993; Nicollet et al. 1997). Recent petrological and geochronological investigations in the Andriamena unit and corresponding basement demonstrate the superposition of three thermal events: 2.5 Ga, 790–730 Ma, and 530–500 Ma (Guérrot et al. 1993; Nicollet et al. 1997; Tucker et al. 1999; Kröner et al. 2000). The Andriamena unit consists of tonalitic and granodioritic gneisses emplaced between 2.55 and 2.50 Ga in an older sequence, which consist of interlayered metapelitic migmatites, quartzites, mafic and quartzofeldspathic gneisses (Tucker et al. 1999; Collins et al. 2001; Collins and Windley 2002). This basement is characterised by small lenses of magnesian granulites, which preserve evidences of UHT metamorphism (Goncalves 2002). These lenses of magnesian granulites preserve petrographical and geochronological evidences along the complex thermal imprint. This Archaean basement is reworked by a middle Neoproterozoic (790–730 Ma) thermal event, which involves emplacement of voluminous maficultramafic bodies accompanied by high-grade metamorphism under upper amphibolite to granulite conditions (Goncalves et al. 2001). This latter event was interpreted as the result of magmatic underplating in a continental magmatic arc setting (Handke et al. 1999; Tucker et al. 1999). At 530–500 Ma, the Andriamena unit experienced a limited overprint under amphibolitic conditions. The nappe emplacement and its final geometry are related to this Cambrian event (Goncalves 2002), which results from crustal shortening during the final amalgamation of Gondwana.

Four magnesian granulites from the Andriamena unit (see location in Fig. 1) have been selected for U-Pb dating. Petrology and metamorphic evolution of the studied samples have been described elsewhere (Goncalves 2002) and will only be summarised here.

Sample C43 preserves a UHT assemblage, which consists of garnet, Al-rich orthopyroxene (Al_2O_3~9 wt%), sapphirine and sillimanite. Peak P-T conditions are 1,050 ± 50 °C and 11.5 ± 0.5 kbar. Peak metamorphism was followed by isothermal decompression of about 4 kbar at 900–950 °C under anhydrous conditions, supported by the local development of coronitic and symplectitic textures composed of cordierite, sapphirine, spinel and orthopyroxene at the expense of the primary phases. Based on EMP data, Goncalves et al. (2001) suggest that such isothermal decompression is an apparent petrographic path, which resulted from the superposition of two distinct events. The primary UHT assemblage was partially reequilibrated during a second event at lower pressure (~7 kbar, 900 °C). Isobaric cooling follows the reequilibration at low pressure, as illustrated by the partial breakdown of the sapphirine-cordierite assemblage into a thin symplectite consisting of orthopyroxene and sillimanite.

Sample C1 also preserves evidences of UHT conditions, which are supported by the occurrence of relictic garnet, Al-rich orthopyroxene, sillimanite and quartz. In contrast to sample C43, retrogression is more developed and occurred under fully hydrated conditions, leading to a secondary orthoamphibole and cordierite-bearing assemblage.

Sample C6 is a strongly retrogressed and deformed magnesian granulite, which mainly consists of orthoamphibole, cordierite, sillimanite and quartz. Primary UHT phases like garnet and orthopyroxene are retrogressed and occur as relics. Metamorphic evolution and thermobarometric estimates suggest that both orthoamphibole-bearing rocks (C1 and C6) cooled from ~7–8 kbar and 900 °C to ~5 kbar and 650 °C.

Sample An6e was collected close to the Brieville village, in the centre of the Andriamena unit (Fig. 1). This rock is an orthoamphibole and cordierite-bearing granulite of highly magnesian bulk composition, similar to samples C1 and C6 dated by conventional methods. The peak metamorphic assemblage consists in relictic garnet (grt_1), orthopyroxene (opx_1), abundant quartz and minor sillimanite (sil_1). This assemblage is typical of UHT conditions, which have been constrained at 11.5 ± 1.5 kbar and 1,050 ± 50 °C by similar rocks (Goncalves et al. 2000). The UHT assemblage is retrogressed by a secondary hydrated assemblage consisting of large euhedral orthoamphibole ($oamph_2$), cordierite (crd_2) and biotite (bt_2). This assemblage is characteristic of amphibolite facies conditions (~6 kbar; 650 °C). Relics of primary garnet (grt_1) are systematically separated from quartz by coronitic textures composed of orthoamphibole, cordierite ± biotite, consistent with the reaction:

$$grt_1 + qtz + H_2O = oamph_2 + crd_2.$$

Analytical techniques

The analytical procedure comprises three stages: (1) characterisation of monazite grains in thin section including the determination of textural relationships and chemical U-Th-Pb ages using EMP, (2) extraction of monazites from thin section by micro-drilling and (3) ID-TIMS dating of the extracted monazites. The method is not more time consuming than the conventional procedure including crushing and mineral separation from large rock samples. This technique is well suited for small and rare samples because only the drilled parts of the thin sections are destroyed.

– (1) Preliminary EMP characterisation was performed using 150 μm thin-section and a Cameca SX 100 electron microprobe with four-wavelength dispersion spectrometer detectors. Backscattered electron imaging was used to find the monazites location and identify textural features and internal zoning. Monazite dating was performed according to a modified version of the analytical procedure detailed by Montel et al. (1996). EMP allowed a quick investigation of the age populations and heterogeneities within individual monazite grains. Individual EMP chemical ages were calculated from the U, Th and Pb concentrations assuming that unradiogenic lead in the monazite is negligible and that no partial lead loss occurred since its initial crystallisation or last complete resetting (closed system evolution). Thus, all the chemical ages should be considered as

apparent ages. U-Th-Pb age population is represented as a weighted histogram corresponding to the sum of all individual ages and their uncertainties. The calculated mean age and its associated 2σ error is based on a least-squares modelling, which allow to identify potential multiple age populations. The quality of the modelling is assessed from the mean square weighted deviation (MSWD).

- (2) Based on petrographic features and EMP results, monazites were extracted from thin-sections using a Medenbach micro-drill mounted on an optical microscope. Figure 2 illustrates successive stages of monazite micro-drilling. Monazites as small as 60 μm have been micro-drilled. During the drilling, surrounding brittle minerals chipped out at the monazite boundary, leaving clean crystals even when the drilling diameter was slightly larger than the monazite. Extracted grains were individually transferred in Petri dishes under binocular microscope, washed with Milli-Q ultrapure water and dried with distilled ethanol.
- (3) Sample dissolution, chemical separation and mass spectrometry follows the technique described in Paquette and Pin (2001). Total Pb blank were 5.5 ± 3.5 pg for Pb and less than 1 pg for U during the analytical period. The U-Pb isotopic results were performed on a FISONS VG Sector 54–30 mass spectrometer in a multicollector static mode, ^{204}Pb was simultaneously measured with a Daly detector ion-counting system. Individual fraction ellipse errors (2σ) and regression calculations were determined using the PbDat 1.24 and Isoplot/Ex 2.49 programs, respectively (Ludwig 1993, 2001). Age uncertainties are quoted at the 2σ level. The decay constants used for the U-Pb system are those determined by Jaffrey et al. (1971) and recommended by the IUGS (Steiger and Jäger 1977).

Conventional ID-TIMS dating results

Before using the micro-drilling sampling technique, conventionally separated zircons and monazites from three samples were first analysed.

Sample C43

In this sample, the zircon grains are light pink with a rounded shape. This morphology was already observed in zircon recrystallised under granulite-facies conditions (Vavra et al. 1996; Schaltegger et al. 1999). Monazite grains are large (>100 μm), anhedral with a honey yellow colour.

Four of the five analysed zircon fractions (Table 1) are discordant and define a discordia line (MSWD = 2.0) with a $2{,}709 \pm 4$ Ma upper intercept and a poorly defined 829 ± 41 Ma lower intercept (Fig. 3a). Two monazite grains are discordant. They plot on quite opposite location in the Concordia diagram (Table 1 and Fig. 3a) and define an upper intercept at $2{,}507 \pm 2$ Ma and a lower intercept at 790 ± 7 Ma. The fifth zircon fraction roughly plots along the chord defined by the monazite analyses. This latter fraction was not characterized by any peculiar observation on the U and Pb concentration or grains colour and shape.

Sample C1

The zircon grains display the same morphology as C43, but are colourless to pale yellow and translucent to brown and turbid crystals. Two types of monazite were observed: mostly ovoid yellow grains and few anhedral yellow-greenish crystals.

Three of the six analysed zircon fractions (Table 1 and Fig. 3b), corresponding to the colourless grains, are concordant to slightly discordant (4 to 8%) and

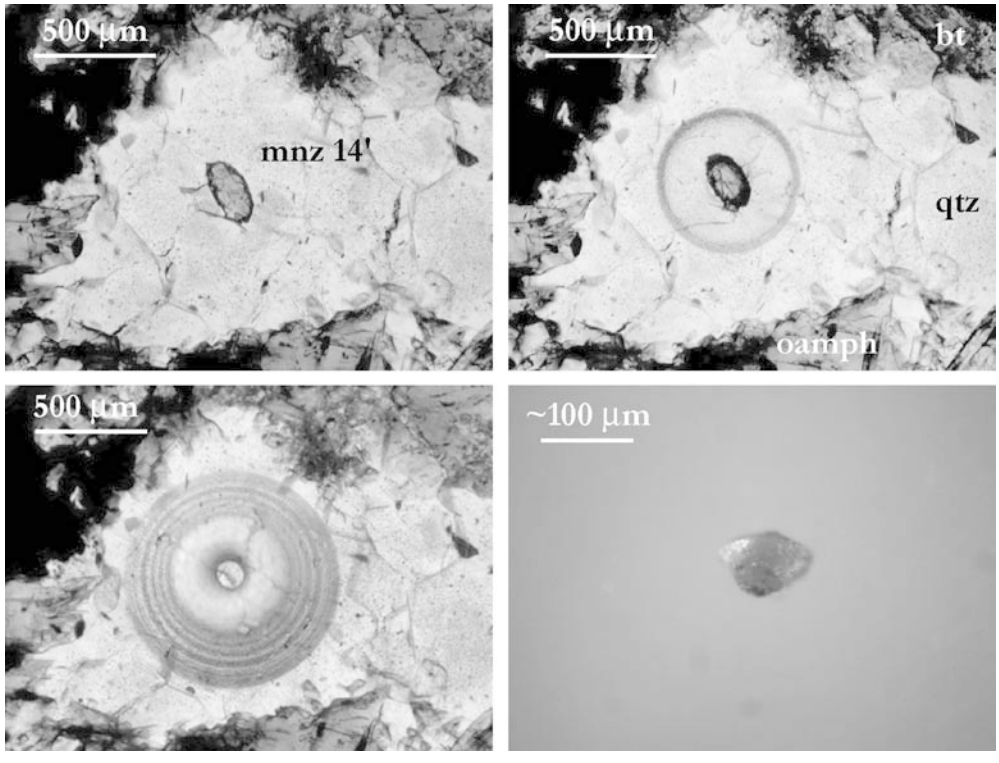

Fig. 2 Photomicrographs illustrating the successive stages of monazite extraction from a thin-section using a Medenbach micro-drill mounted on a conventional optical microscope

Table 1 U-Pb isotope analysis of zircon and monazite from Andriamena UHT granulite C1, C6 and C43

Number	Description	Weight (mg)	Number of grains	Concentrations		Atomic ratios				Apparent ages (Ma)		
				U (ppm)	Pb rad. (ppm)	$^{206}Pb\ ^{204}Pb$	$^{206}Pb/^{238}U \pm 2\sigma$ (%)	$^{207}Pb/^{235}U \pm 2\sigma$ (%)	$^{207}Pb/^{206}Pb \pm 2\sigma$ (%)	$^{206}Pb\ ^{238}U$	$^{207}Pb\ ^{235}U$	$^{207}Pb\ ^{206}Pb$
C43												
Z1	Transp p pi	0.110	1	267	151	152,622	0.5045 ± 0.25	12.851 ± 0.25	0.1847 ± 0.03	2,633	2,669	2,696
Z2	Transp p pi	0.089	1	254	132	32,772	0.4701 ± 0.16	11.759 ± 0.16	0.1814 ± 0.03	2,484	2,585	2,666
Z3	Transp p pi	0.160	2	215	111	111,069	0.4560 ± 0.16	11.313 ± 0.16	0.1799 ± 0.03	2,422	2,549	2,652
Z4	Transp p pi	0.204	2	292	144	48,099	0.4279 ± 0.29	10.438 ± 0.29	0.1769 ± 0.03	2,297	2,474	2,624
Z5	Transp p pi	0.142	2	301	111	45,131	0.3278 ± 0.20	6.621 ± 0.20	0.1465 ± 0.03	1,828	2,062	2,305
Mo1	Anhe ye	0.015	1	1,494	4,776	50,448	0.3883 ± 0.23	8.315 ± 0.23	0.1553 ± 0.03	2,115	2,266	2,405
Mo2	Anhe ye	0.071	1	1,790	4,701	118,928	0.2358 ± 0.47	4.121 ± 0.47	0.1267 ± 0.03	1,365	1,659	2,053
C1												
Z6	Transp clrls	0.034	3	359	199	58,756	0.5165 ± 0.12	13.201 ± 0.13	0.1854 ± 0.03	2,684	2,694	2,702
Z7	Transp clrls	0.040	4	542	290	127,470	0.5025 ± 0.27	12.759 ± 0.27	0.1842 ± 0.03	2,625	2,662	2,691
Z8	Transp clrls	0.022	8	189	105	7,261	0.4950 ± 0.29	12.529 ± 0.29	0.1836 ± 0.06	2,592	2,645	2,685
Z9	Transp p ye	0.069	8	476	246	151,071	0.4861 ± 0.13	12.148 ± 0.13	0.1812 ± 0.03	2,554	2,616	2,664
Z10	Transp ye	0.046	10	451	224	27,587	0.4691 ± 0.18	11.371 ± 0.19	0.1758 ± 0.03	2,479	2,554	2,614
Z11	Turbid br	0.039	7	250	113	12,331	0.4253 ± 0.14	9.629 ± 0.15	0.1642 ± 0.04	2,285	2,400	2,499
Mo3	Round ye	0.004	1	1,481	8,151	11,648	0.4815 ± 0.24	11.177 ± 0.24	0.1683 ± 0.03	2,534	2,538	2,541
Mo4	Round ye	0.015	1	1,292	10,091	28,149	0.4827 ± 0.60	11.206 ± 0.60	0.1684 ± 0.03	2,539	2,540	2,542
Mo5	Anhe ye gr	0.004	1	1,640	3,945	11,822	0.3199 ± 0.17	6.632 ± 0.17	0.1503 ± 0.03	1,790	2,064	2,350
Mo6	Anhe ye gr	0.010	1	780	1,692	21,141	0.2467 ± 0.19	4.524 ± 0.19	0.1330 ± 0.03	1,422	1,735	2,138
Mo7	Anhe ye gr	0.016	1	98.5	647	1,546	0.2405 ± 0.76	4.320 ± 0.90	0.1302 ± 0.44	1,389	1,697	2,101
C6												
Z12	Transp p ye	0.040	16	238	121	4,529	0.4553 ± 0.15	10.651 ± 0.16	0.1697 ± 0.04	2,419	2,493	2,554
Z13	Transp p ye	0.024	12	309	141	2,109	0.4249 ± 0.20	9.799 ± 0.20	0.1673 ± 0.05	2,283	2,416	2,531
Z14	Turbid br	0.029	4	1,124	466	4,839	0.3948 ± 0.13	8.910 ± 0.13	0.1637 ± 0.03	2,145	2,329	2,494
Z15	Turbid br	0.047	4	697	282	3,670	0.3810 ± 0.15	8.502 ± 0.15	0.1618 ± 0.03	2,081	2,286	2,475
Mo8	Anhe ye	0.040	1	90.8	856	8,420	0.1299 ± 0.27	1.173 ± 0.35	0.0654 ± 0.22	788	788	789
Mo9	Anhe ye	0.024	1	37.1	291	2,291	0.1299 ± 0.42	1.174 ± 0.71	0.0655 ± 0.55	787	789	792
Mo10	Round ye	0.047	1	259	3,288	4,068	0.1301 ± 0.91	1.175 ± 0.94	0.0655 ± 0.26	788	789	790

Individual analyses were performed on the least magnetic (2° forward and side tilt at 2.2 A using a Frantz Isodynamic magnetic barrier separator) mechanically abraded and crack-free zircon grains. Monazite grains were not abraded. The isotopic ratios are corrected for mass discrimination (0.1 ± 0.015% per amu for Pb and U), isotopic tracer contribution and analytical blanks: 5.5 ± 3.5 pg for Pb and less than 1 pg for U. Initial common Pb is determined for each fraction in using the Stacey and Kramers (1975) two-step model. Abbreviations: *trans* transparent; *p pi* pale pink; *ye* yellow; *clrls* colourless; *p ye* pale yellow; *br* brown; *anhe* anhedral; *gr* greenish

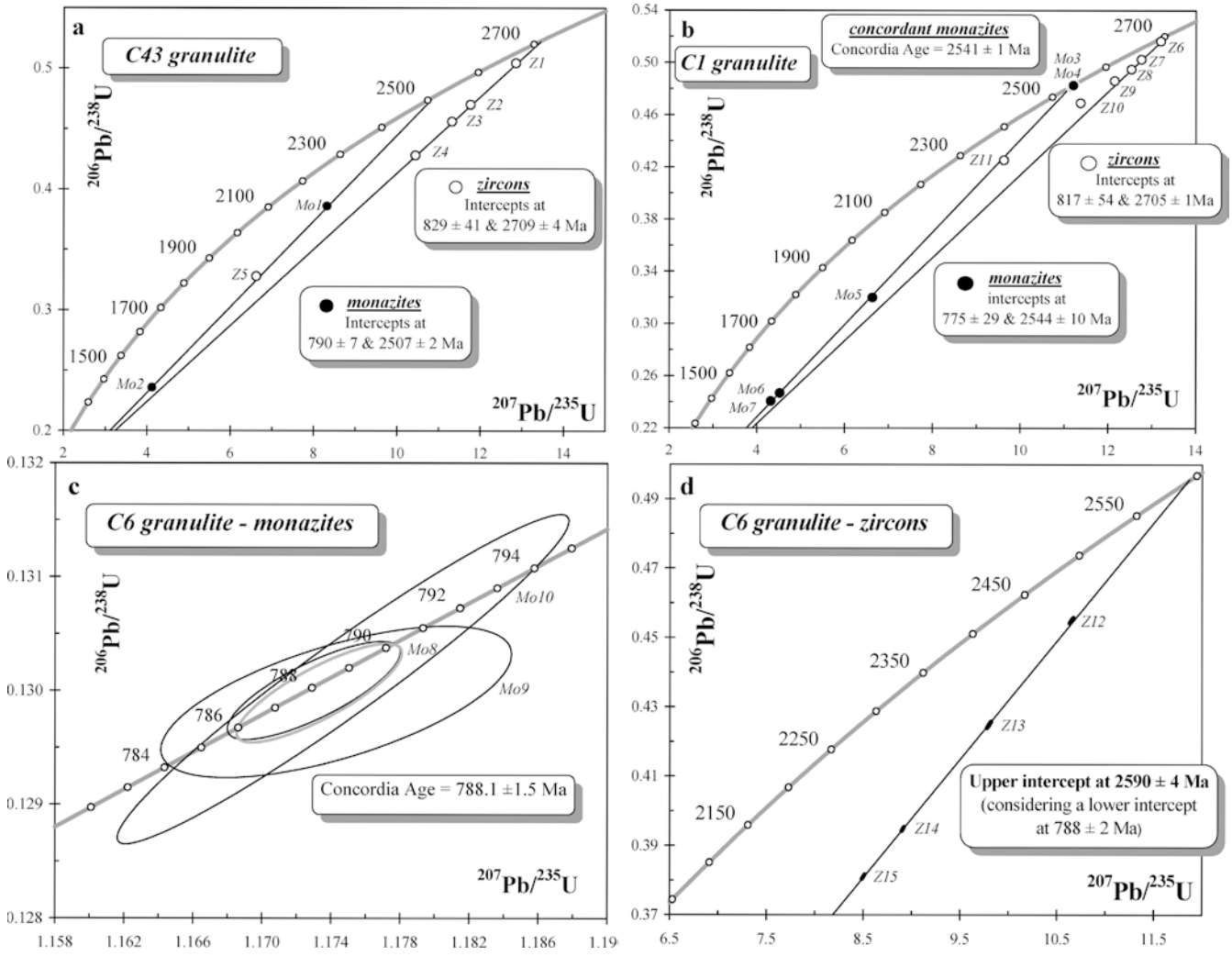

Fig. 3 $^{206}Pb/^{238}U$ vs. $^{207}Pb/^{235}U$ concordia diagrams of conventional multi-grain analysis of zircons and monazites from Andriamena granulites

define a discordia line with an upper intercept at 2,705 ± 1 Ma and a lower intercept at 817 ± 54 Ma (MSWD = 1.4). The three last fractions (Z9, 10, 11) corresponding to the coloured zircons do not fall on a chord and consequently do not provide any meaningful age constraint. The rounded and yellow monazite are concordant at 2,541 ± 1 Ma (Table 1 and Fig. 3b) whereas the three anhedral greenish grains are strongly discordant (46% to 69%). When plotted on the same diagram, the five monazite crystals plot on a poorly-defined alignment (MSWD = 41) with an upper intercept at 2,544 ± 10 Ma and a lower intercept at 775 ± 29 Ma.

Sample C6

The zircon grains are comparable to those of samples C1 and C43. Monazites are translucent, yellow, mostly anhedral and rarely ovoid.

Three analysed monazite crystals are concordant and record a precise age of 788 ± 2 Ma (Fig. 3c and Table 1). The four analysed zircon fractions are discordant along a chord with an upper intercept at 2,588 ± 15 Ma and a lower intercept at 776 ± 100 Ma (Fig. 3d and Table 1). The high MSWD value (MSWD = 21) indicates that the resulting ages are statistically meaningless. If the lower intercept is forced by 788 ± 2 Ma, as defined by the monazite dating, the upper intercept becomes 2,590 ± 4 Ma.

In summary of this first part of the study, conventional U-Pb dating of (mostly single) zircons and monazites recorded three ages, respectively 2.7 Ga, 2.5–2.6 Ga and 790 Ma. Note that only one zircon fraction is concordant (Z6 in sample C1). Half of the analysed monazite grains are also discordant. Two crystals are concordant at 2.54 Ga in sample C1 and the three analysed monazites from sample C6 are all concordant at 790 Ma. At this stage of the study, the interpretation of dating results is speculative. Based on the deformation associated to hydrous retromorphic evolution experienced by sample C6, the 790 Ma-age recorded by concordant monazites can be interpreted as a metamorphic event that has fully reset their U-Pb

isotopic system. Note that this 790 Ma age is more or less precisely dated as lower intercept by zircons and/or monazites in all samples, which favours this hypothesis. Zircon fractions of samples C43 and C1 define upper intercepts at 2,705–2,710 Ma. This age is not recorded by monazites we analysed, thus we suggest this last date represents the igneous emplacement of the granulite protoliths. Finally, a 2.5–2.6 Ga event has been recorded by monazites from C43 and C1. The main problem concerns the interpretation of this last age based on monazites only that may represent a magmatic and/or metamorphic event. The timing of the UHT metamorphic event represents a major constrain for the geological evolution of the Andriamena Complex. The conventional U-Pb dating indicates two possible ages, 790 Ma or 2.5 Ga, but we cannot favour one or the other. Finally, it is difficult to interpret the discordance of the analysed monazites with the results presented here.

In situ ID-TIMS dating results on monazites

To try to solve both questions: age of UHT metamorphism and behaviour of the U-Pb system of the monazites, it is necessary to add spatial resolution to ID-TIMS dating in order to establish a close connection between age and textural location of monazites. In this chapter, we present a new sampling approach for conventional ID-TIMS U-Pb dating of minerals.

Monazite petrography and EMP Th-Pb chemical dating

Monazite is abundant in sample An6e (more than 10 grains > 50 μm per thin section). Three populations of monazite have been distinguished and micro-drilled according to their textural position and crystallographic features.

The first population consists of monazites included in primary garnet (grt_1) that are euhedral micro-inclusions and rounded grains (M12') (Fig. 4a–b). These latter are either fully armoured by garnet or connected with the matrix via numerous cracks within garnet. The euhedral shape of some of these monazites favours a crystallisation coeval with garnet growth under UHT metamorphism.

The second population of monazites (M18', M4', M17, M2') is located into the matrix which consists of aggregated and recrystallised quartz grains (Fig. 4c). They occur as included or interstitial grains. Most of these monazites display an ovoid morphology with homogeneous or core-rim internal structure. Monazite M2' displays a zoning with two different chemical domains bounded by internal euhedral crystallographic faces.

The third population represents the main occurrence of monazites in sample An6e. It was found in the hydrated coronitic textures formed at the expense of garnet (Fig. 4d). These large grains (> 100 μm) display a very irregular shape, potentially resulting from the combined growth of both monazite and hydrated mineral assemblage. Monazites from hydrated zones display either no

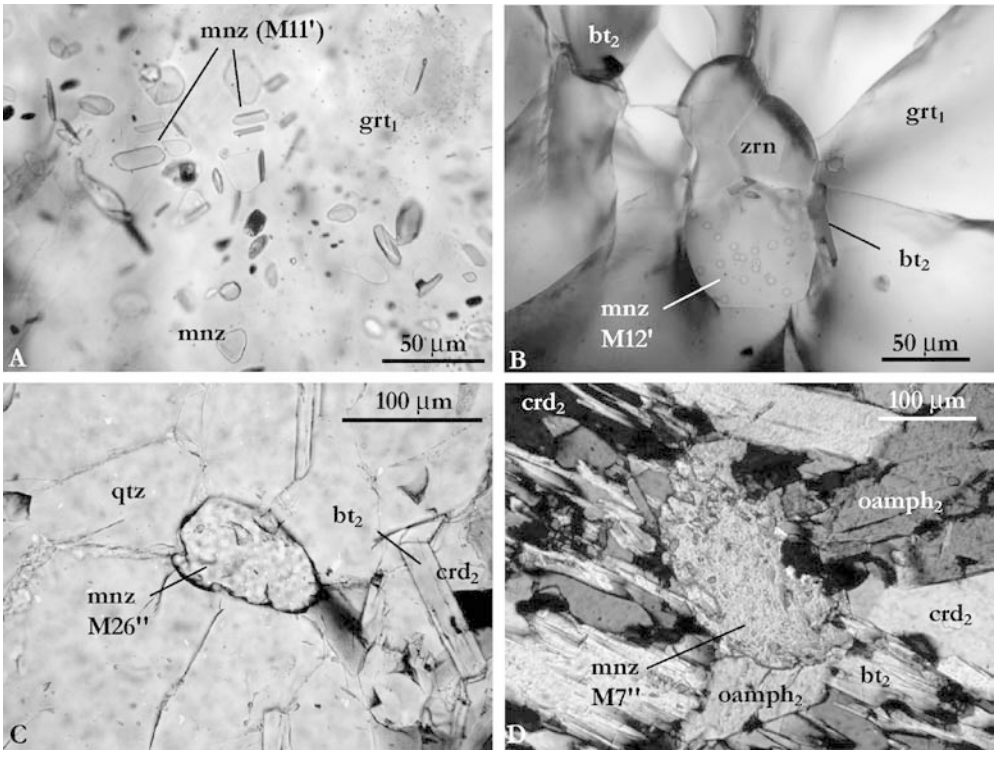

Fig. 4 Photomicrographs showing the distinct populations of monazites and their textural features from sample An6e. **A** Fully armoured euhedral micro-inclusions included in a primary UHT garnet. **B** Rounded grain of monazite, associated with three zircons, included in a primary UHT garnet. The monazite is connected with the matrix via numerous garnet cracks. **C** Monazite located in the matrix composed of an aggregate of recrystallized equant polygonal grains of quartz. **D** Monazite located into the secondary hydrated aggregates of orthoamphibole, cordierite and biotite. They are characterized by an irregular shape that may have resulted from intergrowth with the host-hydrated minerals. The core of the grain is totally inclusion free in contrast to the rim

internal zoning or a core-rim structure. The rims contain numerous euhedral inclusions of quartz, orthoamphibole, cordierite and biotite, which confirms that the growth of monazite rims is coeval with garnet breakdown during the retrograde evolution.

One common feature to all monazite populations (in quartz, in hydrated aggregates and in garnet connected to the matrix by cracks) is the frequent occurrence of small overgrowths or internal dark domains located close to inclusions.

The ages obtained by EMP U-Th-Pb dating of monazites from sample An6e are scattered, considering the different crystal populations (Fig. 5) or within single grains (Goncalves 2002) (Fig. 6). In the three monazite occurrences, garnet, quartz and hydrated coronitic reactions, the measured ages are more often generally continuously distributed between 2.5 and 0.75 Ga (Fig. 5). The oldest apparent ages were recorded in monazites located in primary garnet porphyroblasts and in a lesser extend in the quartz matrix (Fig. 5a–b). In contrast, monazites located in the secondary coronitic textures yield younger ages with a minimum value around 0.75 Ga (Fig. 5c). This scatter may result from the combination of lead loss and monazite growth episodes as suggested by the occurrence of inherited cores surrounded by recrystallised rims. Most of these monazites are also characterized by the occurrence of small overgrowth and internal domains dated around 500 Ma (Figs. 5 and 6d). The homogeneity of the youngest population and the fact that no intermediate ages between 750 and 500 Ma have been reported, suggests that the Cambrian event is meaningful. Two important geochronological information can be derived from this part. At first, the Th-Pb isotopic system of the studied monazites is discordant at the scale of the EMP spot size (~3 μm). Consequently, the U-Pb dating results obtained by ID-TIMS at the grain scale will also be discordant. Furthermore, the studied monazites are composite and do not display concentric structures. They comprise old cores, recrystallized domains, late overgrowths and patches located in the inner parts of the grains.

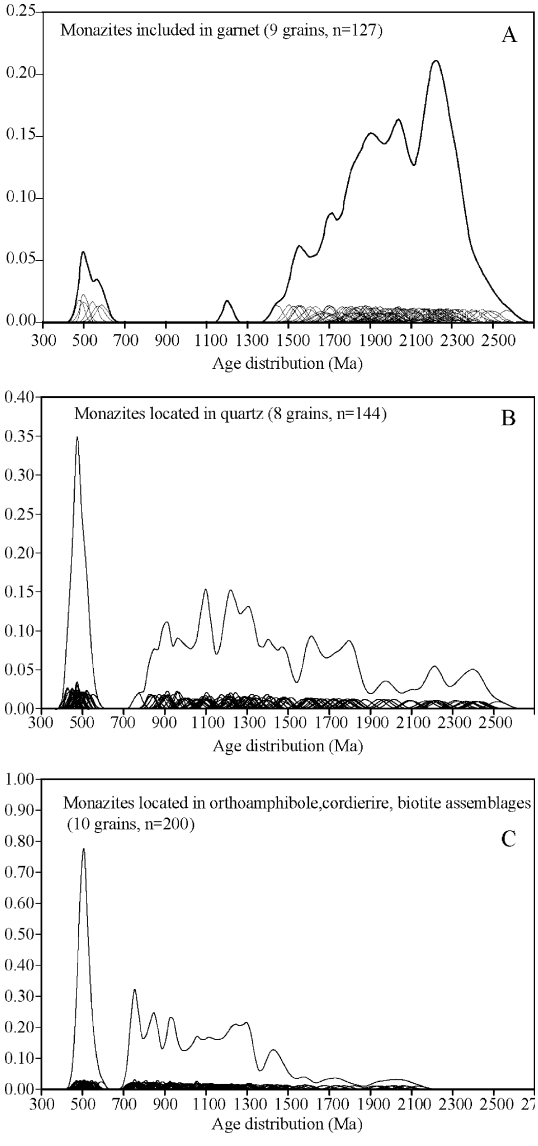

Fig. 5 Weighted-histogram representations of the U-Th-Pb chemical age data of monazite included in garnet, quartz and hydrated aggregates from sample An6e (Goncalves 2002). The ordinate consists of unit-free values representing the sum of the Gaussian curves

ID-TIMS U-Pb dating of micro-drilled single monazites

Twelve monazite grains were selected and micro-drilled for individual dating. The results are reported on a Concordia diagram (Fig. 7 and Table 2), where individually analyzed monazites all plot on discordant trajectories, from 13 to 95%. Considering that all these monazites are extracted from thin sections of a single sample, their relative location on the Concordia diagram tend to be connected to their textural position within the mineralogical assemblage. Consequently, the different results and corresponding ages are discussed relatively to the textural location of the monazites.

- (1) The two monazites included in garnet (M8, M12) produce comparable and moderately discordant (29–32%) analytical points which indicate $^{207}Pb/^{206}Pb$ apparent ages of 2.4 Ga.
- (2) Three grains were located within the coronitic domains (M10, M16, M'5). The analytical points are strongly discordant, from 70 to 95%. A fourth one (M9'), characterised by a comparable level of discordance, plots on a distinct trajectory and suggests an older lower intercept than the other monazites. The near lack of Cambrian domains within this grain was emphasized by the EMP study (Fig. 6c).
- (3) Three grains were located into the matrix at the contact between recrystallised quartz and hydrated coronitic assemblages (M3, M4, M17). These points are strongly discordant, from 75 to 83%, and plot

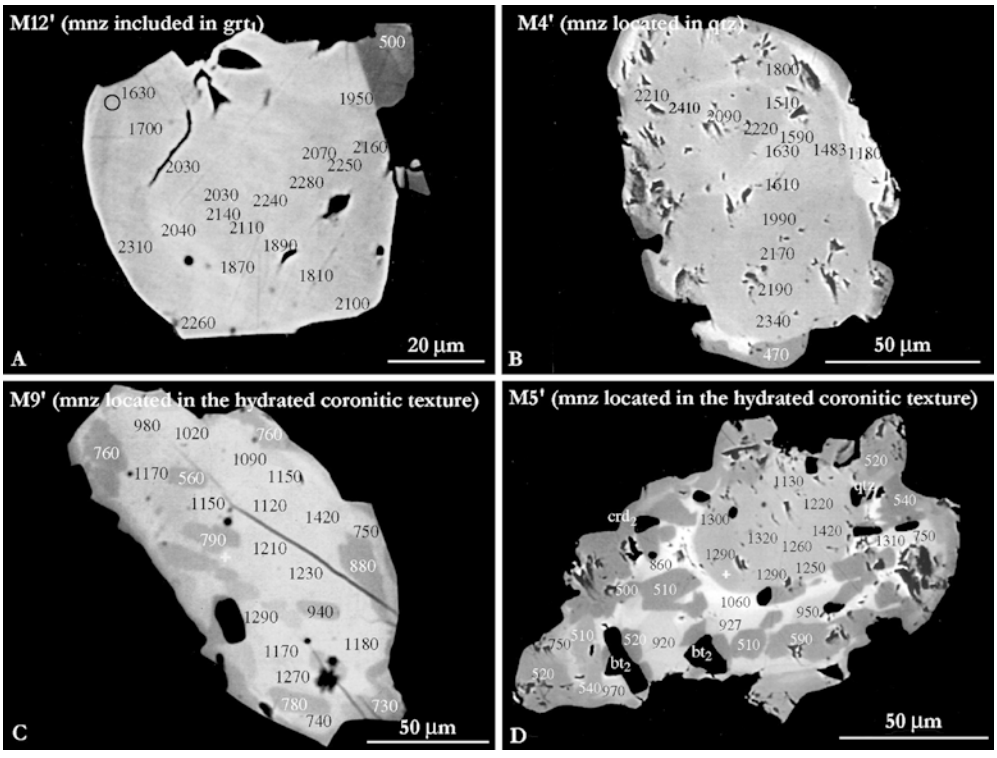

Fig. 6 Back-scattered electron images and corresponding mapping of U-Th-Pb chemical ages of monazites located in different textural positions: in garnet (**A**), in quartz (**B**), in hydrated coronitic textures (**C** and **D**). Typical individual errors are 30–50 Ma for 0.5–1.0 Ga ages, 50–70 Ma for 1.0–2.0 Ga ages and 70–90 Ma for 2.0–2.7 Ga ages

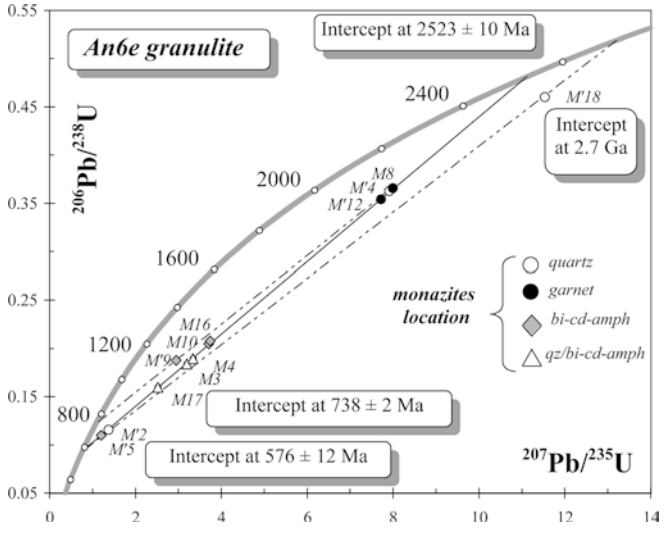

Fig. 7 $^{206}Pb/^{238}U$ vs. $^{207}Pb/^{235}U$ concordia diagram of micro-drilled monazites from the Andriamena granulite An6e. Each monazite grain is characterized by its textural position

near the monazites located within the coronitic domains only.

– (4) The three last grains, included into quartz, display contrasted U-Pb systematics. Monazite M18' is much less discordant than the other crystals (13%) and preserved a pre-metamorphic history of the protolith at 2.7 Ga. Grain M4' is moderately discordant (30%) and plots closely to the garnet-included monazites. Note that M4' and M5' grains (Fig. 6b, c) were separated by 1.5 mm only on the thin section. Grain M2' is highly discordant (94%) and plots near monazite M5' located within the coronitic domains, both grains being characterised by large Cambrian overgrowths (see Fig. 6d for M5').

Ten of the twelve analysed monazite plot on an imperfect alignment, corresponding to garnet-hosted monazites on the one side and to monazites located within garnet breakdown products on the other side. Calculation using a model 2-fit (Ludwig 2001) indicates two intercepts with the Concordia curve at 2,523 ± 10 Ma and 576 ± 12 Ma, respectively (Fig. 7). Additionally, a line joining M8 (monazite included in garnet) and M9' (Cambrian overgrowth-free monazite sample) allows to calculate an upper intercept at 2.56 Ga and a lower intercept at 740 Ma, which confirms the near lack of Cambrian overprint in the M9' grain. Finally, a regression line starting from the 576 Ma lower intercept and including the oldest M18' monazite indicates a probable 2.7 Ga upper intercept age.

Interpretation of dating results and discussion

Most of the monazites from the matrix are constituted of one or several old cores and recrystallised domains dated between 2.5 and 0.75 Ga with the frequent occurrence of 500 Ma overgrowths and/or inner patches (Fig. 5). Consequently, ID-TIMS dating of such complex crystals cannot result in perfectly defined discordia line because the proportion of each component vary from grain to grain. Accordingly, the lower intercepts calculated at 740 and 576 Ma only represent minimum

Table 2 U-Pb isotope analysis of zircon and monazite from Andriamena UHT granulite An6e

Number	Description	Weight (mg)	Number of grains	Concentrations		Atomic ratios				Apparent ages (Ma)		
				U (ppm)	Pb rad. (ppm)	^{206}Pb ^{204}Pb	$^{206}Pb/^{238}U$ $\pm 2\sigma$ (%)	$^{207}Pb/^{235}U$ $\pm 2\sigma$ (%)	$^{207}Pb/^{206}Pb$ $\pm 2\sigma$ (%)	^{206}Pb ^{238}U	^{207}Pb ^{235}U	^{207}Pb ^{206}Pb
An6e												
M'18	Quartz	0.011	1	1,189	6,681	52,690	0.4605 ± 0.12	11.532 ± 0.12	0.1816 ± 0.03	2,442	2,567	2,668
M'4	Quartz	< 0.001	1	1,506	8,866	6,813	0.3618 ± 0.19	8.177 ± 0.21	0.1639 ± 0.09	1,991	2,251	2,496
M'2	Quartz	< 0.001	1	564	2,083	559	0.1159 ± 1.36	1.371 ± 1.96	0.0858 ± 1.33	707	876	1,334
M8	Garnet	0.013	1	900	4,290	13,576	0.3660 ± 0.53	7.991 ± 0.53	0.1584 ± 0.03	2,011	2,230	2,438
M'12	Garnet	< 0.001	1	2,081	7,337	10,635	0.3542 ± 0.14	7.710 ± 0.15	0.1579 ± 0.06	1,954	2,198	2,433
M16	Bi-cd-amph	0.001	1	3,704	10,735	6,263	0.2079 ± 0.17	3.743 ± 0.19	0.1306 ± 0.08	1,218	1,581	2,106
M10	Bi-cd-amph	< 0.001	1	3,703	7,147	6,524	0.2046 ± 0.15	3.705 ± 0.17	0.1313 ± 0.08	1,200	1,572	2,116
M'9	Bi-cd-amph	0.001	1	7,080	12,745	10,846	0.1876 ± 0.13	2.945 ± 0.14	0.1139 ± 0.05	1,108	1,394	1,862
M'5	Bi-cd-amph	< 0.001	1	1,294	3,007	1,314	0.1101 ± 0.63	1.203 ± 0.94	0.0793 ± 0.66	673	802	1,179
M4	Qz/bi-cd-am	< 0.001	1	475	3,854	591	0.1899 ± 2.40	3.342 ± 2.88	0.1277 ± 1.48	1,121	1,491	2,066
M3	Qz/bi-cd-am	< 0.001	1	987	5,717	2,214	0.1838 ± 0.41	3.194 ± 0.49	0.1260 ± 0.25	1,088	1,456	2,043
M17	Qz/bi-cd-am	0.001	1	1,138	6,058	591	0.1598 ± 0.50	2.518 ± 0.73	0.1143 ± 0.49	956	1,277	1,869

Monazite grains were not abraded. The isotopic ratios are corrected for mass discrimination (0.1 ± 0.015% per amu for Pb and U), isotopic tracer contribution and analytical blanks: 5.5 ± 3.5 pg for Pb and less than 1 pg for U. Initial common Pb is determined for each fraction in using the Stacey and Kramers (1975) two-step model. Abbreviations: *bi-cd-amph* biotite-cordierite-orthoamphibole; *qz/bi-cd-amph* at the limit between quartz and biotite-cordierite-orthoamphibole assemblages

and maximum estimates, respectively. All the data plot into a triangle with an upper pole at 2.52–2.54 Ga and lower poles at 790 Ma (ID-TIMS on C6 monazites) and 520 Ma (EMP on An6e). ID-TIMS dating has shown that all the monazites from sample An6e were discordant at least at the single grain scale. Most of the ages determined by EMP are ranging from 2.5 to 0.75 Ga, which implies that the Th-Pb chronometer also provides discordant ages, possibly resulting from old and young micro-domains, in spite of the reduced EMP spot size. The well-defined 500-Ma peaks suggest that the U-Th-Pb Cambrian ages measured by EMP on overgrowths are probably meaningful. Finally, a single monazite grain armoured in quartz was almost fully preserved from three metamorphic overprints and confirms the occurrence of a 2.7 Ga igneous protolith age, previously determined by ID-TIMS dating of zircons from samples C1 and C43. Consequently, a total of four ages appear to be recorded by U-Pb systematic on monazite grains from a single thin-section.

The conventional U-Pb dating was unable to constrain the age of the UHT metamorphism: 790 Ma or 2.5 Ga? This question was answered through dating micro-drilled monazites in textural equilibrium with UHT garnet (sample An6e). Consequently, the late Archaean event (~2.5 Ga) is identified as the age of the UHT metamorphism (1,050 ± 50 °C and 11.5 ± 1.5 kbar). UHT granulites occurred as small lenses that were strongly reworked during Neoproterozoic times. The lack of structural markers makes the geodynamic context at the origin of this high-grade event unconstrained. The UHT granulites were affected by a second metamorphic event under lower granulite facies conditions (900 °C and ~7 kbar) at 790 Ma (ID-TIMS on C6 monazites). This event is characterized by the breakdown of the UHT garnet into a hydrated orthoamphibole and cordierite-bearing assemblage. The age of the retrogression is consistent with one drilled monazite (M'9 in Fig. 6) located in the hydrated coronitic textures. This second episode of monazite growth was produced by dissolution-precipitation as illustrated by the occurrence of UHT cores surrounded by rims containing mineral products from the breakdown of the UHT assemblage. This granulite event is coeval with the emplacement of voluminous mafic rocks and granitoids in Central and North-Central Madagascar interpreted as arc magmatism related to the closure of the Mozambique ocean (Guérrot et al. 1993; Handke et al. 1999; Tucker et al. 1999, Kröner et al. 2000). The large diachrony between the UHT peak metamorphism and the subsequent hydrated retrogression (2.5 Ga–790 Ma) is noticeable. These new geochronological constraints demonstrate that the metamorphic evolution of the investigated rocks cannot be interpreted as the result of a single thermal event.

The fourth thermal event, dated around 500 Ma, is characterized by the formation of small overgrowths and of recrystallized domains pervasively distributed throughout the grains (Fig. 6d). This last episode of

monazite growths was mostly recorded using the high spatial resolution of the EMP since the overgrowths are more often lower than 10 μm in size (Figs. 5 and 6d). In addition, Cambrian ages are also recorded from recrystallized monazite domains located at the contact with silicate inclusions (quartz, cordierite, biotite, orthoamphibole) or in garnet cracks (Fig. 6a). Consequently, we suggest that this Cambrian recrystallization episode may be related to fluid circulation. This latter event is coeval with the emplacement and deformation of the Andriamena unit at 530–500 Ma (Goncalves et al. 2003), under upper amphibolite facies conditions (5–7 kbar, 650–700 °C). The deformation is probably connected to the continental convergence of the Australia-Antarctica block and Madagascar-Sri Lanka-South India-East Africa block during the final amalgamation of Gondwana. The absence or weak imprint of this Cambrian event in the Mg-granulites may be partly due to their refractory behaviour, to the localized nature of fluid circulations and to lowest metamorphic conditions.

The EMP characterization and "in situ" ID-TIMS dating on thin sections from sample An6e demonstrate that most monazites from the matrix display various age domains interpreted as resulting from distinct episodes of monazite growth or recrystallization during metamorphic events (2.5 Ga, 790 and 500 Ma). Consequently, the observed discordance of ID-TIMS data points mainly reflects a mixture of different domains that crystallized at different times. Nevertheless, EMP also revealed that the studied monazites were discordant (Fig. 6) at the scale of the spot-size (~3 μm), which implies that mixing of old and young components also appear at the micrometer scale. The second episode of monazite growth occurred at 790 Ma and was produced by dissolution-precipitation as illustrated by the occurrence of UHT cores surrounded by rims containing minerals from the breakdown of the UHT assemblage (Fig. 6d). The discordance level of the analysed monazites reported in the Concordia diagram is correlated to their textural position. Monazite included into garnet is less discordant due to the shielding effect of garnet (Montel et al. 2000). Monazites located in quartz display discordance degrees from 13 to 94%, depending on their position in the middle or at the border of the grain, where the sensitivity to fluid interactions increases. The preservation of a weakly-discordant age of 2.7 Ga in a single monazite grain, despite the superposition of several metamorphic events, one of which occurring under high-grade thermal conditions (~1,050 °C), demonstrates the robustness of the U-Pb system of monazites in the absence of fluid circulation. This also confirms suggests that quartz, in favourable cases, may have the same shielding effect than garnet (e.g. Hawkins and Bowring 1997; Poitrasson et al. 2002). In contrast, monazites located in the hydrated coronitic textures (orthoamphibole, biotite and cordierite) and in the matrix at the contact with cordierite are the most discordant. We suggest that this fluid-rich environment probably favours dissolution-precipitation and consequently isotope resetting. Likewise, the Cambrian episode of monazite (re)crystallization could also result from dissolution-precipitation process related to fluid interactions. According to Seydoux-Guillaume et al. (2002), dissolution-precipitation processes are particularly efficient under Ca-rich fluid conditions favouring the brabantite substitution ($Ca,Th(PO_4)_2$). Interestingly, the Cambrian overgrowths are significantly enriched in Ca suggesting the activity of a possible Ca-enriched fluid.

Numerous recent studies illustrate that monazite geochronology is sometimes more complex then generally assumed. This is related to the widespread recrystallization of discrete domains pervasively distributed throughout the grains (e.g. Townsend et al. 2000). This type of mechanism often caused isotopic discordance of analysed monazites (e.g. Crowley and Ghent 1999). When the initially closed U-Pb system of monazites is disturbed by a single event, then a combined study using ID-TIMS and EMP on mineral separates can provide precise constraints on the age and origins of the discordance (Crowley and Ghent 1999). Another powerful approach is the combination of SIMS U-Th-Pb dating associated to EMP chemical study of monazites, both on thin sections (Foster et al. 2000). In the studied An6e sample, the monazites were affected by at least two distinct metamorphic events and single grains were all discordant in the Concordia diagram. In such a case, a careful evaluation of the analytical strategy is required. (i) First, U-Pb or U-Th-Pb dating allows to plot the results in the two-dimensions Concordia diagram, where discordance level, alignment and intercept ages are easier to decipher than using frequency histograms. (ii) Second, the possibility to produce "in situ" dating (in thin sections) rather using monazite concentrates allows to associate petrographic textures to geochronological results. In this study, the link between monazite U-Pb age and host minerals and paragenesis provides helpful constraints. The careful examination and Th-Pb chemical dating of monazites in thin sections using EMP produces the mapping of compositions and apparent ages for each grain. This provides key information for monazite selection before micro-drilling and ID-TIMS dating. (iii) Finally, considering the extreme heterogeneity at the micrometer scale of An6e monazite grains where the SIMS potentialities cannot be fully exploited, then ID-TIMS on micro-drilled monazites is a valuable approach as illustrated in this study. Based on the whole set of data, mixing micro-drilled monazites from thin sections and mineral separates, we significantly improved our understanding of the timing of UHT granulites from Madagascar.

Conclusions

Four ages were obtained by combined EMP and ID-TIMS U-Pb dating of micro-drilled monazites on a single UHT granulite from Central Madagascar.

Combined with conventional U-Pb results on zircon and monazite separates from three adjacent samples, this "in situ" dating allows us to propose the following evolution. The oldest and most probably primary igneous event is recorded at 2.7 Ga by zircons and one quartz-shielded monazite grain. The Ultra High Temperature metamorphism is defined at 2.5 Ga by both garnet-included monazites and mineral separates. Two later events are recorded, the first at 790 Ma in (1) micro-drilled monazites included into hydrated retrograde assemblages and (2) in monazites from strongly deformed C6 sample. The second event is dated at 500 Ma, mostly by EMP on thin overgrowths and/or pervasively recrystallized domains.

This article is an attempt to demonstrate the potentialities of the "in-situ" U-Pb dating technique of micro-drilled monazite crystals to unravel complex poly-metamorphic evolutions and to put absolute time constraints on P-T paths. This technique represents, when its application is possible, an interesting opportunity combining precise ID-TIMS U-Pb dating and EMP petrographic characterisation. The major interest is the possibility to put time constraints on geological processes at the thin section scale, the main drawback being the difficulty to obtain concordant intercept ages at the single grain scale when the monazites have recorded numerous events.

Acknowledgments P.G. fieldwork was financially supported by the "Service des Relations Internationales" from the Université Blaise Pascal, Clermont-Ferrand. Many thanks are also due to the laboratoire de Géologie of the University of Antananarivo (Madagascar) for their logistic support. The authors are grateful to Elizabeth J. Catlos, Urs Schaltegger and Franck Poitrasson for their helpful and advisable comments.

References

Braun I, Montel JM, Nicollet C (1998) Electron microprobe dating of monazite from high-grade gneisses and pegmatites of the Kerala Khondalite Belt, southern India. Chem Geol 146:65–85

Catlos EJ, Gilley LD, Harrison TM (2002a) Interpretation of monazite ages obtained via in situ analysis. Chem Geol 188:193–215

Catlos EJ, Harrison TM, Manning CE, Grove M, Rai SM, Hubbard MS, Upreti BN (2002b) Records of the evolution of the Himalayan orogen from in situ Th-Pb ion microprobe dating of monazite: eastern Nepal and western Garhwal. J Asian Earth Sci 20:459–479

Cocherie A, Legendre O, Peucat JJ, Kouamelan AN (1998) Geochronology of polygenetic monazites constrained by in situ electron microprobe Th-U-total lead determination; implications for lead behaviour in monazite. Geochim Cosmochim Acta 62:2475–2497

Collins AS, Windley BF (2002) The tectonic evolution of Central and Northern Madagascar and its place in the final assembly of Gondwana. J Geol 110:325–339

Collins AS, Windley BF, Kröner A, Fitzsimons I, Hulscher B (2001) The tectonic architecture of central Madagascar: implication on the evolution of the East African Orogeny. Gond Res 4:152–153

Copeland P, Parrish RR (1988) Identification of inherited radiogenic Pb in monazite and its implications for U-Pb systematics. Nature 333:760–763

Crowley JL, Ghent ED (1999) An electron microprobe study of the U-Th-Pb systematics of metamorphosed monazite; the role of Pb diffusion versus overgrowth and recrystallization. Chem Geol 157:285–302

DeWolf CP, Belshaw NS, O'Nions RK (1993) A metamorphic history from micron-scale $^{207}Pb/^{206}$ Pb chronometry of Archean monazite. Earth Planet Sci Lett 120:207–220

Foster G, Gibson HD, Parrish R, Horstwood M, Fraser J, Tindle A (2002) Chemistry and physics of accessary minerals; crystallisation, transformation and geocronological applications. Chem Geol 191:183–207

Foster G, Kinny P, Vance D, Prince C, Harris N (2000) The significance of monazite U-Th-Pb age data in metamorphic assemblages; a combined study of monazite and garnet chronometry. Earth Planet Sci Lett 181:327–340

Goncalves P (2002) Pétrologie et Géochronologie des Granulites de Ultra-Hautes Températures de l'unité basique d'Andriamena (Centre Nord Madagascar). Unpublished PhD Thesis, Université de Clermont-Ferrand, France, 320 pp

Goncalves P, Nicollet C, Lardeaux JM (2000) In-situ electron microprobe monazite dating of the complex retrograde evolution of UHT granulites from Andriamena (Madagascar): apparent petrographical path vs. PTt path. Geol Soc Am, Annual Meeting, Reno, USA. Geol Soc Am Abstracts with Programs 32

Goncalves P, Nicollet C, Lardeaux JM (2003) Finite strain pattern in Andriamena unit (North-Central Madagascar): evidence for late Neoproterozoic-Cambrian thrusting during continental convergence. Precambrian Res 123:135–157

Goncalves P, Nicollet C, Montel JM, Lefevre B, Paquette JL, Lardeaux JM, Pin C (2001) Is the petrographical PTt path consistent with the real thermal path? The example of the polymetamorphic Ultra-High Temperature granulites of Andriamena (Madagascar). EUG XI, Strasbourg, France. Terra Abstract 12

Guerrot C, Cocherie A, Ohnenstetter M (1993) Origin and evolution of the West Andriamena Pan-African mafic-ultramafic complex in Madagascar as shown by U-Pb, Nd isotopes and trace element constraints. EUG VIII, Starsbourg, France. Terra Abstract 5:387

Handke MJ, Tucker RD, Ashwal LD (1999) Neoproterozoic continental arc magmatism in west-central Madagascar. Geology 27:351–354

Harrison TM, Grove M, Lovera OM, Catlos EJ, D'Andrea J (1999) The origin of Himalayan anatexis and inverted metamorphism; models and constraints. J Asian Earth Sci 17:755–772

Harrison TM, McKeegan KD, LeFort P (1995) Detection of inherited monazite in the Manaslu leucogranite by $^{208}Pb/^{232}Th$ ion microprobe dating; crystallization age and tectonic implications. Earth Planet Sci Lett 133:271–282

Hawkins DP, Bowring SA (1997) U-Pb systematics of monazite and xenotime; case studies from the Paleoproterozoic of the Grand Canyon, Arizona. Contrib Mineral Petrol 127:87–103

Jaffrey AH, Flynn KF, Glendenin LE, Bentley WC, Essling AM (1971) Precision measurement of half-lives and specific activities of ^{235}U and ^{238}U. Phys Rev C4:1889–1906

Kober B (1986) Whole-grain evaporation for $^{207}Pb/^{206}Pb$-age-investigations on single zircons using a double-filament thermal ion source. Contrib Mineral Petrol 93:482–490

Kober B (1987) Single-zircon evaporation combined with Pb+ emitter bedding for $^{207}Pb/^{206}Pb$-age investigations using thermal ion mass spectrometry, and implications to zirconology. Contrib Mineral Petrol 96:63–71

Kouamelan AN, Delor C, Peucat JJ (1997) Geochronological evidence for reworking of Archean terrains during the early Proterozoic (2.1 Ga) in the western Cote d'Ivoire (Man Rise-West African Craton). Precambrian Res 86:177–199

Kröner A, Hegner E, Collins AS, Windley BF, Brewer TS, Razakamanana T, Pidgeon RT (2000) Age and magmatic history of the Antananarivo block, central Madagascar, as derived from zircon geochronology and Nd isotopic systematics. Am J Sci 300:251–288

Ludwig KR (1993) Pbdat: a computer program fro processing Pb-U-Th isotope data, version 1.24. US Geological Survey, Open-File Report 88–542, 32 pp

Ludwig KR (2001) User manual for Isoplot/Ex rev. 2.49. A geochronological toolkit for Microsoft Excel. Berkeley Geochronology Center Spec Publ no 1a, 56 pp

Montel JM, Foret S, Veschambre M, Nicollet N, Provost A (1996) Electron microprobe dating of monazite. Chem Geol 131:37–53

Montel JM, Kornprobst J, Vielzeuf D (2000) Preservation of old U-Th-Pb ages in shielded monazite: example from the Beni Bousera Hercynian kinzigites (Morocco). J Metamorph Geol 18:335–342

Nicollet C, Montel JM, Foret S, Martelat JE, Rakotondrazafy R, Lardeaux JM (1997) E-Probe monazite dating in Madagascar: a good example of the usefulness of the in-situ dating method. UNESCO-IUGS-IGCP 348/368. Internal Symposium and field workshop on proterozoic geology of Madagascar, MADAGASCAR. Abstract, 65

Overstreet WC (1967) The geologic occurrence of monazite. US Geol Surv Prof Pap Rep 0530, 327 pp

Paquette JL, Pin C (2001) A new miniaturized extraction chromatography method for precise U-Pb zircon geochronology. Chem Geol 176:311–319

Parrish RR (1990) U-Pb dating of monazite and its application to geological problems. Can J Earth Sci 27:1431–1450

Poitrasson F, Hanchar JM, Schaltegger U (2002) The current state and future of accessory mineral research. Chem Geol 191:3–24

Schaltegger U, Fanning CM, Guenther D, Maurin JC, Schulmann K, Gebauer D (1999) Growth, annealing and recrystallization of zircon and preservation of monazite in high-grade metamorphism; conventional and in-situ U-Pb isotope, cathodoluminescence and microchemical evidence. Contrib Mineral Petrol 134:186–201

Schärer U, Xu Rong-Hua, Allègre CJ (1986) U-(Th)-Pb systematics and ages of Himalayan leucogranites, South Tibet. Earth Planet Sci Lett 77:35–18

Seydoux-Guillaume AM, Paquette JL, Wiedenbeck M, Montel JM, Heinrich W (2002) Experimental resetting of the U-Th-Pb system in monazite. Chem Geol 191:165–181

Steiger RH, Jäger E (1977) Subcommission on geochronology: convention to use of decay constants in geo and cosmochronology. Earth Planet Sci Lett 26:207–221

Stern RA (1997) The GSC sensitive high resolution ion microprobe (SHRIMP): analytical techniques of zircon U-Th-Pb age determinations and performance evaluation. Radiogenic age and isotopic studies. Report 10 Geol Surv Can Curr Res:1–31

Stern RA, Berman RG (2001) Monazite U-Pb and Th-Pb geochronology by ion microprobe, with an application to in situ dating of an Archean metasedimentary rock. Chem Geol 172:113–130

Stern RA, Sanborn N (1998) Monazite U-Pb and Th-Ph geochronology by high-resolution secondary ion mass spectrometry; in Radiogenic age and isotopic studies. Rep 11 Geol Surv Can Curr Res, pp 1–18

Townsend KJ, Miller CF, D'Andrea JL, Ayers JC, Harrison TM, Coath CD (2000) Low temperature replacement of monazite in the Ireteba granite, Southern Nevada: geochronological implications. Chem Geol 172:95–112

Tucker RD, Ashwal LD, Handke MJ, Hamilton MA, Le Grange M, Rambeloson RA (1999) U-Pb geochronology and isotope geochemistry of the Archean and Proterozoic rocks of north-central Madagascar. J Geol 107:135–153

Vavra G, Gebauer D, Schmid R, Compston W (1996) Multiple zircon growth and recrystallization during polyphase Late Carboniferous to Triassic metamorphism in granulites of the Ivrea Zone (Southern Alps); an ion microprobe (SHRIMP) study. Contrib Mineral Petrol 122:337–358

Williams ML, Jercinovic MJ (2002) Microprobe monazite geochronology: putting absolute time into microstructural analysis. J Struct Geol 24:1013–1028

Zhu XK, O'Nions RK, Belshaw NS, Gibb AJ (1997a) Significance of in situ SIMS chronometry of zoned monazite from the Lewisian granulites, Northwest Scotland. Chem Geol 135:35–53

Zhu XK, O'Nions RK, Belshaw NS, Gibb AJ (1997b) Lewisian crustal history from in situ SIMS mineral chronometry and related metamorphic textures. Chem Geol 136:205–218

Zhu XK, O'Nions RK, Gibb AJ (1998) SIMS analysis of U-Pb isotopes in monazite: matrix effects. Chem Geol 144:305–312